The rise and fall of proboscidean ecological diversity

Authors: Juan L. Cantalapiedra[1], Óscar Sanisidro[1], Hanwen Zhang[2,3], María T. Alberdi[4], José L. Prado[5], Fernando Blanco[6], Juha Saarinen[7].

[1] Universidad de Alcalá, GloCEE – Global Change Ecology and Evolution Research Group, Departamento de Ciencias de la Vida, 28805, Madrid, Spain.
[2] School of Earth Sciences, University of Bristol, Wills Memorial Building, Queens Road, Bristol, BS8 1RJ, United Kingdom.
[3] Department of Earth Sciences, Natural History Museum, Cromwell Road, London, SW7 5BD, United Kingdom.
[4] Departamento de Paleobiología, Museo Nacional de Ciencias Naturales (CSIC), José Gutiérrez Abascal 2, 28006 Madrid, Spain.
[5] INCUAPA, CONICET-UNICEN. Universidad Nacional del Centro de la Provincia de Buenos Aires. Del Valle 5737. B7400JWI- Olavarría, Argentina.
[6]Museum für Naturkunde, Leibniz-Institut für Evolutions- und Biodiversitätsforschung, Invalidenstr. 43, 10115 Berlin, Germany.
[7] Department of Geosciences and Geography, University of Helsinki, FI-00014, Helsinki, Finland.

*Correspondence to: jlopezcant@gmail.com

Abstract

Proboscideans were keystone Cenozoic megaherbivores, and present a highly relevant case study to frame the tempo and magnitude of recent megafauna extinctions against long-term macroevolutionary patterns. Surveying the entire proboscidean fossil history using model-based approaches, we show that the dramatic Miocene explosion of proboscidean functional diversity was triggered by their biogeographic expansion beyond Africa. Ecomorphological innovations drove niche differentiation, and communities that accommodated several disparate proboscidean species in sympatry became commonplace. The first burst of extinctions took off in the Late Miocene (~ 7 Ma). Importantly, this and subsequent extinction trends show high

ecomorphological selectivity, and went hand-in-hand with palaeoclimate dynamics. The global extirpation of proboscideans began escalating from 3 Ma with further extinctions in Eurasia, and then a dramatic increase in Africa extinctions at 2.4 Ma. Overhunting by humans may have served as a final double jeopardy in the Late Pleistocene, following climate-triggered extinction trends that began long before hominins evolved suitable hunting capabilities.

Main text

The worldwide extirpation of megafaunas was a radical upheaval in the recent evolutionary history of terrestrial ecosystems, with Late Pleistocene human activities often considered culpable[1,2]. Yet, understanding these extinctions in view of long-term macroevolutionary dynamics of the megafauna lineages has been critically lacking[3]. Proboscideans, being keystone megaherbivores in Cenozoic terrestrial ecosystems, were among the most affected groups. For centuries[4,5], their fossil record has elucidated an evolutionary history of success and decline in equally dramatic measures, with three endangered living elephant species[6] representing a mere vestige of a once formidable clade high in both taxonomic diversity and ecomorphological disparity, spread across Africa, Eurasia and the Americas. Therefore, proboscidean evolution poses an invaluable case study for palaeobiologists to explore causes of uneven distribution in biodiversity across phylogeny and evolutionary history. Hereby, we comprehensively re-examine the rich fossil record of proboscideans in its entirety, and investigate the interactions between proboscidean diversification and the tempo and mode of their ecomorphological evolution. Our approach assesses clade and community-level dynamics, placing emphasis on the timing and processes behind the sudden decimation of this group in the Quaternary. Our research presents a blueprint for evaluating any plausible impact of Pleistocene humans on megafauna extinctions[1] against long-term macroevolutionary factors of decline.

We compiled a dataset for extinct and living proboscidean taxa with unprecedented detail, consisting of 185 species, 2,130 fossil occurrences and 17 ecomorphological traits (including body size, craniodental morphology, mode of mastication, tusk morphology, and foot posture; see Extended Data Fig. 1), which are pertained to multiple fundamental aspects of proboscidean functional ecology (e.g. breadth of dietary preference and feeding envelope, food processing, energy requirements, home range, social grouping, sexual selection, and mode of locomotion). Based on these traits, and through nonmetric multidimensional scaling (NMDS) analysis, we

constructed a two-dimensional functional morphospace of proboscideans that condenses 93% of their ecomorphological variation (Fig. 1b). A first empirical dimension of proboscidean functional morphospace (NMDS-1) encapsulates greater dental masticatory durability (DMD), through increasing mesiodistal length, number of transverse loph(id)s, and relative crown height (degree of hypsodonty) of the molars. These trends eventually facilitated dentitions with a high proal shearing effectiveness during mastication, key to enhanced dietary plasticity and processing of low-quality food[7–9]. A second dimension reflects larger-scale craniodental modifications, including but not limited to: development of sharp or obtuse dental loph(id)s, curvature of upper tusks, presence of shovel-like lower tusks and elongated mandible (Extended Data Fig. 2). This functional space yields eight proboscidean functional types (PFTs), each representing a cluster of ecomorphologically similar species, and thus experiencing similar evolutionary pressures[10] (Fig. 1a-c, and Extended Data Fig. 2 and 3). We reconstruct the global and continental diversification trajectories of proboscideans based on occurrence data[11], and use multidimensional phylogenetic models[12] to assess the mode of evolution of lineages across the above-mentioned functional space (see below). We inspect mechanisms behind community assembly and disassembly processes using general linear mixed-effects models (see methods).

Early diversification and the dispersal outside Afro-Arabia

During the first half of their history, until some 30 Ma, proboscideans were restricted to Afro-Arabia. Species diversity across this interval rose steadily, but with no substantial ecological diversification, and only two out of the eight PFTs evolved. Despite a good coverage in the Early Eocene fossil record, initial diversification rate estimates should be read with caution given a sizable gap in the record between around 51 and 40 Ma (see the broad 95% credibility intervals in Fig. 1d). But, from then on, our estimates show that net diversification remained high compared to other mammalian clades[13,14] (average diversification was 0.08 species/Myr; see Fig. 1d). In fact, this rate was sustained until the collapse of the group in the Quaternary (Fig. 1d). Importantly, our global diversification estimates aggregate clade-wise rate variations, and do not imply rate homogeneity across lineages and geographic regions (Fig. 1d). With diversity doubling every 9 Myr on average, we found little evidence of an asymptotic global carrying capacity constraining proboscidean diversity (Extended Data Fig. 4), a scenario where speciation and extinction rates are expected to balance each other rendering zero net diversification[15]. The

absence of a global diversity limit in proboscideans is likely the result of processes operating at different scales: geographic expansion, local niche partitioning, and ecology-dependent species survival.

The latest Oligocene and Early Miocene (25 to 20 Ma) witnessed the expansion of several proboscidean lineages beyond of Afro-Arabia (termed 'Proboscidean Datum Event' by students of Eurasian biochronology[16] or PDE; Fig. 1c). Current understanding of proboscidean evolution emphasises the importance of the PDE, since following this bio-event proboscideans became ubiquitous in megaherbivore guilds across Eurasia as well as Africa[16–18]. Around 16 Ma, proboscideans incurred into North America, setting a new biogeographic milestone. Alongside the progressive increase in seasonality and landscape heterogeneity during the Neogene[19], major biogeographic events like the PDE are expected to increase clades' global carrying capacity[20], boosting speciation opportunities[21] and phenotypic evolution[22], stemming from the exposure to a wider array of environmental settings and biotic interactions. However, the impact of the PDE on proboscidean macroevolutionary patterns has never been quantified. To further explore the relevance of the PDE, we use multidimensional phylogenetic procedures[12] to test scenarios of unconstrained, decelerating, and constrained evolution, as well as a suite of models where African lineages evolved in a different fashion to those evolving in other continents (see Methods). The best fit model shows that rates of ecomorphological evolution in African lineages were slow and ameliorated over time (Extended Data Fig. 5), underlining the modest ecological diversity of African lineages before the Neogene. Lineages outside Africa, on the other hand, evolved 25 times faster (Extended Data Fig. 5). The inception of Eurasian lineages triggered unprecedented radiation in both diversity and disparity of proboscideans, culminating in the establishment and expansion of several new PFTs (Fig. 1c).

Local and clade-scale patterns

The Neogene expansion outside Africa drastically changed the course of proboscidean evolution, both in their global and local diversity and disparity. The sustained emergence of functional novelties translated into niche differentiation in proboscideans, facilitating faunas which accommodated several sympatric proboscidean species[23,24]. Linear models offer an insight into trends in local proboscidean diversity, and how this relates to the masticatory functional morphology of the constituent proboscidean taxa (see methods). Before the PDE, alpha diversity

remained relatively low. But following the PDE — around 22 Ma — and until 8 Ma, African and Eurasian faunas were overall richer in proboscidean species, and this richness generally increased over time (Extended Data Fig. 6). Over this period, community-level diversity is significantly correlated with higher local mean NMDS-1 value (P = 0.004; Extended Data Fig. 7). Proboscideans responsible for this signal were the PFT 5 (e.g., amebelodonts or "shovel-tuskers") and PFT 6 (e.g., stegolophodonts) taxa, which underwent evolutionary modifications towards enhanced DMD, as well as divergent feeding biomechanics (i.e., enlarged functional lower incisors in PFT 5[25], and foreshortened jaws for greater mechanical efficiency of mastication in PFT 6[9]). Higher prevalence of these functionally specialised taxa reduced the intensity of interspecific competition, allowing herbivore guilds to accommodate more proboscidean species.

In sum, increasing global ecomorphological diversity, combined with niche partitioning in sympatric proboscidean species, produced high initial speciation rates in Eurasia and the Americas, and also fuelled sustained net diversification in Africa. Together with the poor performance of phylogenetic models where ecomorphological evolution decelerates as a function of time (Extended Data Fig. 5), the multilayer approach presented here reinforces an expansionist scenario of global proboscidean diversification, mediated by geographic dispersals, amelioration of local competition, and relentless exploration of different functional ecomorphological adaptations.

Local processes also impacted proboscidean macroevolutionary patterns via ecology-mediated diversification. The dynamic and heterogeneous late Neogene and Quaternary biospheres imposed more austere resource limitations, accelerating the evolution of multi-loph(id) dentition optimised for effective proal shearing (highest DMD) in stegodonts and elephantids (PFTs 7 and 8)[9,26]. As testified by successive peripatric speciation events during the evolution of mammoths[27,28], novel adaptive responses of peripheral populations to marginal conditions[21] played a key role in the diversification of PFT 7 and PFT 8 taxa. At the broadest scale, our ecology-dependent diversification models[14] reveal that these taxa with further increasing DMD[9] show higher macroevolutionary persistence, signified by higher speciation rate and moderate extinction risk (Fig. 2, Extended Data Fig. 8 and 9), a finding consistent with the rapid expansion of PFTs 6, 7 and 8 in the late Neogene and Quaternary (Fig. 1c). Furthermore, ecology-selective

survivorship alone (species sorting) is a macroevolutionary force capable of influencing evolutionary trends[29], and has probably been a major factor propelling lineages into unexplored regions of the proboscidean functional space.

Late Neogene turnover

The onset of C_4 grass-dominated habitats around 8 Ma, which brought about less productive and markedly seasonal conditions[30], brought dramatic changes to the evolutionary context of megafauna communities[26,31]. After the C_4 shift, proboscidean communities began to deplete. Our community-level analyses depict a sustained decrease of local proboscidean richness over time (Extended Data Fig. 6 and 7), as decreasing productivity in seasonal savannah-grassland biomes[32] could not sustain multiple competitively robust proboscidean species with further enhanced DMD and greater foraging flexibility[8,33,34]. For the first time, herbivore guilds dominated by these new PFTs (6, 7 and 8) contain fewer proboscidean species than those with more ecomorphologically disparate proboscidean assemblages ($P < 0.001$). Through most of the Neogene, extinction was highly biased towards the more archaic proboscidean taxa with primitive dentition (Extended Data Fig. 10). In the Late Miocene, extinctions eroded a broader spectrum of the functional space (Fg. 3b). Deinotheres (PFT 2) and trilophodont gomphotheres (dominant components of PFTs 3 and 5) were major casualties. Interestingly, whereas gomphotheres are characterised by high volatility (high speciation and extinction rates), deinotheres showed remarkable ‘living-fossil’-like macroevolutionary tendencies[35,36], being persistently low in diversity and deficient in apomorphy acquisition (Fig. 1c, 2b).

Meanwhile, the expansion of PFTs 6, 7 and 8 sustained further net positive diversification. Increased climatic perturbations and ecosystem heterogeneity would have promoted allopatric speciation and local selection[21,27,28]. Given the decline of local diversity, the maintenance of global diversity would have stemmed from enhanced taxonomic provinciality between regions (beta diversity). At the macroevolutionary scale, this shift is more clearly reflected in Eurasian diversification trends (Fig. 1d). Around 7 Ma, sustained extinctions produced a brief decline in Eurasian diversity (Extended Data Fig. 4). Eurasian proboscidean diversity managed to recover at around 5 Ma, as speciation rates underwent a four-fold increase and extinction stabilised between 6 and 3 Ma (Fig. 1d).

The Quaternary collapse

With newly-established PFTs showing ample diversification potential, no evidence of a diversity equilibrium being approached (a maximal diversity of 33 species is estimated around 3.2 Ma), and no signal of evolutionary stagnation, nothing would have predicted the abrupt collapse of the clade in Quaternary times[7]. Although speciation rate in Eurasia remained high, extinction aggravated at around 3 Ma, progressively hampering net diversification, as exemplified by the rapid coming and going of numerous dwarfed insular species before the Late Pleistocene. In Africa, extinction rates suddenly quintupled the background Neogene rates around 2.4 Ma (Fig. 2a), a pulse that saw decline in African elephantid (PFT 8 taxa) diversity[37]. These events mark the first phase of broad-scale global proboscidean demise, which first wiped out the few relict PFT 5 species in North America , and then the last deinotheres (PFT 2) in Africa. The axe also reached the brevirostrine gomphotheres (PFT 6) and mammutids (PFT 4), removing broader portions of the functional morphospace than ever before (Fig. 3b). The decimation of proboscidean communities continued (Extended Data Fig. 7). There is a substantial shift towards a higher local mean NMDS-1 from 2.4 Ma onwards (Extended Data Fig. 7), reflecting a wipeout of "mastodont-grade" taxa in Eurasia and Africa and their replacement by PFTs 7 and 8[8,33,38,39]. Yet, the estimated global proboscidean diversity by the end of this first phase was still around 23 species, although a third of which were endemic island dwarfs[40]. A second phase of proboscidean demise is recovered in Eurasia and the Americas, starting ca. 160 and 75 kya, respectively (Fig. 1E). These extinction shifts represent a 24- and 16-fold increase in severity with respect to Neogene basal levels in Eurasia and the Americas, respectively (Fig. 3a). The already severely depleted mammutids and gomphotheres (PFTs 4 and 6) completely disappeared. Proboscideans with the most proal shearing-adapted dentitions (PFTs 7 and 8)[9], which had weathered the first extinction wave, were hit hard too (Fig. 1c and 3b).

The cumulative evidence points to a major role of environmental forcing in the collapse of proboscideans. Extinction severity in Africa and Eurasia during the last 10 Myrs track global temperature trends, according to environment-dependent extinction models[14] (Fig. 3c). Decrease in average global temperature[41] (measured through $\delta^{18}O$) and increase in the amplitude of temperature fluctuations yielded a significant relationship with extinction rates. Our models uncover continent-wide associations of extinction and environmental deterioration, but they do

not imply homogeneity in causality across lineages and smaller geographic scales. Plummeting productivity and ecological reshuffling[42] (including enhanced competition with other ungulate clades that evolved specialist grazing ecomorphs) due to rapid Plio-Pleistocene climatic fluctuations set a tight grip on proboscidean diversity limits, stemming from a sustained decrease in the capacities of ecosystems to support diverse megaherbivore communities throughout the Plio-Pleistocene[31]. Remarkably, the onset of the second, most acute extinction regime is not recovered in Africa, and pre-dates the settlement of *Homo sapiens* in Eurasia and Americas (Fig. 3a). The final dismantling of proboscidean communities and the downfall of the clade was likely initiated by the severe Holarctic climatic changes from the MIS 6 glaciation (ca. 190 kyr) to the particularly harsh and cool climatic conditions of the MIS 4 stadial (ca. 74 kyr). Nevertheless, our results do not contradict a scenario whereby anthropogenic pressure contributed to the further catastrophic decline of proboscideans towards the end of the Pleistocene, as indicated by the timing of extinction of many of the remaining taxa[43,44]. Significantly, some of the shifts in ecosystem functioning that triggered the decline of proboscideans were already in place before they had an obvious impact on diversity trajectories, which highlights the importance of integrating ecomorphological and local-scale approaches when establishing the causes of megafauna declines.

In summary, the fossil evidence shows that proboscidean evolution was a complex and continuous innovative process that allowed this group to overcome 60 million years of severe environmental shifts. The high diversification rate estimated for the clade is consistent with the notion that *K* strategies should promote speciation by ensuring the persistence of marginal populations in new environments[21]. Increasingly resource-efficient ecomorphological novelties would have complemented such strategies, enhancing species persistence and speciation, and in turn propelling ecological innovation. Proboscideans were far from a case of lineage senescence when their demise started, showing that large branches of the tree of life may vanish long before exhausting their evolutionary potential[7,45].

References

1. Surovell, T., Waguespack, N. & Brantingham, P. J. Global archaeological evidence for proboscidean overkill. *Proc National Acad Sci USA* **102**, 6231–6236 (2005).

2. Smith, F. A., Smith, R. E. E., Lyons, S. K. & Payne, J. L. Body size downgrading of mammals over the late Quaternary. *Science* **360**, 310–313 (2018).

3. Faith, J. T., Rowan, J., Du, A. & Barr, W. A. The uncertain case for human-driven extinctions prior to *Homo sapiens*. *Quaternary Res* **96**, 88–104 (2020).

4. Cuvier, G. Mémoires sur les espèces d'éléphants vivants et fossiles. *Mémoires de l'Institut des Sciences et Arts* **2**, 1–22 (1800).

5. Osborn, H. F. The Ancestral Tree of the Proboscidea. Discovery, Evolution, Migration and Extinction Over a 50,000,000 Year Period. *Proc Nat Acad Sci USA* **21**, 404–412 (1935).

6. IUCN. The IUCN Red List of Threatened Species. Version 2021-1. https://www.iucnredlist.org (2021).

7. Maglio, V. J. Origin and Evolution of the Elephantidae. *T Am Philos Soc* **63**, 1 (1973).

8. Zhang, H., Wang, Y., Janis, C. M., Goodall, R. H. & Purnell, M. A. An examination of feeding ecology in Pleistocene proboscideans from southern China (*Sinomastodon*, *Stegodon*, *Elephas*), by means of dental microwear texture analysis. *Quatern Int* **445**, 60–70 (2017).

9. Saegusa, H. Stegodontidae and *Anancus*: Keys to understanding dental evolution in Elephantidae. *Quaternary Sci Rev* **231**, 106176 (2020).

10. Hempson, G. P., Archibald, S. & Bond, W. J. A continent-wide assessment of the form and intensity of large mammal herbivory in Africa. *Science* **350**, 1056–1061 (2015).

11. Silvestro, D., Salamin, N., Antonelli, A. & Meyer, X. Improved estimation of macroevolutionary rates from fossil data using a Bayesian framework. *Paleobiol* **45**, 546–570 (2019).

12. Clavel, J., Escarguel, G. & Merceron, G. mvMORPH: an R package for fitting multivariate evolutionary models to morphometric data. *Methods Ecol Evol* **6**, 1311–1319 (2015).

13. Cantalapiedra, J. L., Fernández, M. H., Azanza, B. & Morales, J. Congruent phylogenetic and fossil signatures of mammalian diversification dynamics driven by Tertiary abiotic change. *Evolution* **69**, 2941–2953 (2015).

14. Silvestro, D., Antonelli, A., Salamin, N. & Quental, T. B. The role of clade competition in the diversification of North American canids. *Proc Nat Acad Sci USA* **112**, 8684–8689 (2015).

15. Sepkoski, J. J. A kinetic model of Phanerozoic taxonomic diversity I. Analysis of marine orders. *Paleobiology* **4**, 223–251 (1978).

16. Tassy, P. The Proboscidean Datum Event: how many proboscideans and how many events? in *European Neogene Mammal Chronology* 237–252 (Plenus Press, 1989). doi:10.1007/978-1-4899-2513-8_16.

17. Made, J. van der. The evolution of the elephants and their relatives in the context of changing climate and geography. in *Elefantentreich - Eine Fossilwelt in Europa* (ed. Meller, H.) (Landesamt für Denkmalpflege und Archäologie Sachsen-Anhalt - Landesmuseum für Vorgeschichte, 2010).

18. Saarinen, J. J. *et al.* Patterns of maximum body size evolution in Cenozoic land mammals: eco-evolutionary processes and abiotic forcing. *Proc Royal Soc B* **281**, 20132049 (2014).

19. Fortelius, M. *et al.* Evolution of Neogene Mammals in Eurasia: Environmental Forcing and Biotic Interactions. *Annu Rev Earth Pl Sc* **42**, 579–604 (2014).

20. Marshall, C. R. & Quental, T. B. The uncertain role of diversity dependence in species diversification and the need to incorporate time-varying carrying capacities. *Phil Trans Roy Soc B* **371**, 20150217–13 (2016).

21. Vrba, E. S. Evolution, species and fossils: how does life evolve? *S. African J. Sci.* **76**, 61–84 (1980).

22. Cantalapiedra, J. L., Prado, J. L., Fernández, M. H. & Alberdi, M. T. Decoupled ecomorphological evolution and diversification in Neogene-Quaternary horses. *Science* **355**, 627–630 (2017).

23. Calandra, I., Göhlich, U. B. & Merceron, G. How could sympatric megaherbivores coexist? Example of niche partitioning within a proboscidean community from the Miocene of Europe. *Naturwissenschaften* **95**, 831–838 (2008).

24. Sanders, W. J. Proboscidea from Kanapoi, Kenya. *J Hum Evol* **140**, 102547 (2020).

25. Wang, S. *et al.* Evolution of Protanancus (Proboscidea, Mammalia) in East Asia. *J Vertebr Paleontol* **35**, e881830 (2015).

26. Lister, A. M. The role of behaviour in adaptive morphological evolution of African proboscideans. *Nature* **500**, 331–334 (2013).

27. Lister, A. M., Sher, A. V., Essen, H. van & Wei, G. The pattern and process of mammoth evolution in Eurasia. *Quatern Int* **126**, 49–64 (2005).

303 28. Wei, G. *et al.* New materials of the steppe mammoth, *Mammuthus trogontherii*, with
304 discussion on the origin and evolutionary patterns of mammoths. *Sci China Earth Sci* **53**, 956–
305 963 (2010).

306 29. Stanley, S. M. *Macroevolution, patterns and processes*. (W.H. Freeman and Company,
307 1979).

308 30. Edwards, E. J. *et al.* The Origins of C4 Grasslands: Integrating Evolutionary and Ecosystem
309 Science. *Science* **328**, 587–591 (2010).

310 31. Faith, J. T., Rowan, J., Du, A. & Koch, P. L. Plio-Pleistocene decline of African
311 megaherbivores: No evidence for ancient hominin impacts. *Science* **362**, 938–941 (2018).

312 32. Kaya, F. *et al.* The rise and fall of the Old World savannah fauna and the origins of the
313 African savannah biome. *Nat Ecol Evol* **2**, 241–246 (2018).

314 33. Saarinen, J. & Lister, A. M. Dental mesowear reflects local vegetation and niche separation
315 in Pleistocene proboscideans from Britain. *J Quaternary Sci* **31**, 799–808 (2016).

316 34. Rivals, F., Semprebon, G. M. & Lister, A. M. Feeding traits and dietary variation in
317 Pleistocene proboscideans: A tooth microwear review. *Quaternary Sci Rev* **219**, 145–153 (2019).

318 35. Vrba, E. S. Evolutionary Pattern and Process in the Sister-Group Alcelaphini-Aepycerotini
319 (Mammalia: Bovidae). in *Living Fossils* (eds. Eldredge, N. & Stanley, S. M.) 62–79 (Springer,
320 1984).

321 36. Herrera-Flores, J. A., Stubbs, T. L. & Benton, M. J. Macroevolutionary patterns in
322 Rhynchocephalia: is the tuatara (*Sphenodon punctatus*) a living fossil? *Palaeontology* **60**, 319–
323 328 (2017).

324 37. Todd, N. E. Trends in Proboscidean Diversity in the African Cenozoic. *J Mamm Evol* **13**, 1–
325 10 (2006).

326 38. Rivals, F., Mol, D., Lacombat, F., Lister, A. M. & Semprebon, G. M. Resource partitioning
327 and niche separation between mammoths (*Mammuthus rumanus* and *Mammuthus meridionalis*)
328 and gomphotheres (*Anancus arvernensis*) in the Early Pleistocene of Europe. *Quatern Int* **379**,
329 164–170 (2015).

330 39. Sanders, W. J. & Haile-Selassie, Y. A New Assemblage of Mid-Pliocene Proboscideans from
331 the Woranso-Mille Area, Afar Region, Ethiopia: Taxonomic, Evolutionary, and Paleoecological
332 Considerations. *J Mamm Evol* **19**, 105–128 (2012).

333 40. Geer, A. A. E. *et al.* The effect of area and isolation on insular dwarf proboscideans. *J*
334 *Biogeogr* **43**, 1656–1666 (2016).

335 41. Westerhold, T. *et al.* An astronomically dated record of Earth's climate and its predictability
336 over the last 66 million years. *Science* **369**, 1383–1387 (2020).

337 42. Vrba, E. S. Habitat Theory in Relation to the Evolution in African Neogene Biota and
338 Hominids. in *African Biogeography, Climate Change, and Hominid Evolution* (eds. Bromage, T.
339 G. & Shrenk, F.) 19–39 (1999).

340 43. Stuart, A. J. Late Quaternary megafaunal extinctions on the continents: a short review. *Geol J*
341 **50**, 338–363 (2015).

342 44. Jukar, A. M., Lyons, S. K., Wagner, P. J. & Uhen, M. D. Late Quaternary extinctions in the
343 Indian Subcontinent. *Palaeogeogr Palaeoclim Palaeoecol* **562**, 110137 (2021).

344 45. Raup, D. M. *Extinction: Bad Genes or Bad Luck?* (Norton, 1991).

345 46. Cantalapiedra, J. L. *et al.* Conserving evolutionary history does not result in greater diversity
346 over geological time scales. *Proc Royal Soc B* **286**, 20182896 (2019).

347 47. Ronquist, F. *et al.* MrBayes 3.2: Efficient Bayesian Phylogenetic Inference and Model
348 Choice Across a Large Model Space. *Systematic Biol* **61**, 539–542 (2012).

349 48. Hublin, J.-J. *et al.* New fossils from Jebel Irhoud, Morocco and the pan-African origin of
350 *Homo sapiens*. *Nature* **546**, 289–292 (2017).

351 49. O'Connell, J. F. *et al.* When did *Homo sapiens* first reach Southeast Asia and Sahul? *Proc*
352 *National Acad Sci* **115**, 8482–8490 (2018).

353 50. Ardelean, C. F. *et al.* Evidence of human occupation in Mexico around the Last Glacial
354 Maximum. *Nature* **584**, 87–92 (2020).

355 51. Paradis, E. *Analysis of Phylogenetics and Evolution with R (Second Edition).* (Springer,
356 2012).

357 52. Revell, L. J. phytools: an R package for phylogenetic comparative biology (and other things).
358 *Methods Ecol Evol* **3**, 217–223 (2012).

359 53. Bates, D., Mächler, M., Bolker, B. & Walker, S. Fitting Linear Mixed-Effects Models Using
360 lme4. *J Stat Softw* **67**, (2015).

361 54. MacLatchy, L. M., Desilva, J., Sanders, W. J. & Wood, B. Hominini. in *Cenozoic Mammals*
362 *of Africa* (eds. Werdelin, L. & Sanders, W. J.) 471–545 (University of California Press, 2010).

363

364

365

Methods

Occurrence dataset

We gathered a species-level occurrence dataset for proboscideans drawn from the literature and online databases. We reviewed the dataset for taxonomic rigour and used the literature to maximise the precision of spatiotemporal occurrence data. Since occurrences with broad temporal ranges flatten diversification rates, we excluded occurrences with broad temporal ranges, unless this significantly decimated the occurrence available for a given taxon (see details in Supplementary Methods).

We retain 1,427 records and 129 species from the NOW database (https://nowdatabase.org/now/database) and 626 records and 33 species from the PBDB (https://paleobiodb.org). A further 73 occurrences for 37 species were added based on an assortment of other published studies. 22 of these species were not originally included in NOW and PBDB, resulting in a 12% increment of the total diversity studied. The final dataset includes 2,130 occurrences for 185 proboscidean species, with an average temporal precision of 1.06 Myr (median 0.8 Myr; 95% CI: 0.002675 — 3.7 Myr).

Phylogenetic dataset

We draw extensively from the pre-existing systematic palaeontological literature, to build an informal proboscidean supertree that incorporates current understanding of their phylogenetic relationships, but at the same time acknowledges the uncertainty —both topological and temporal— derived from all the available sources.

The baseline topology included polytomies where branching relationships between species remain uncertain. We combined this topology with the oldest credible occurrence of each species, and used a tip-dating procedure[46] implemented in MrBayes[47] to generate a posterior distribution of trees that are consistent with all the information available to date, while accounting for temporal and topological uncertainties. From the posterior distribution, 100 trees were retained for further analyses. Further details are provided in the Supplementary Methods.

Functional ecology and proboscidean functional types (PFTs)

Our aim is to capture the evolutionary patterns behind the rise and demise of functional diversity (FD) of proboscideans over time. To delimit different proboscidean functional ecomorphs, we consider functional traits that synthesise morphologies with a clear role in the interactions of each species with its environment, condensing aspects like breadth of dietary preference and feeding envelope, food processing, energy requirements, home range size, social grouping, sexual selection and locomotion. A total of 17 discretised traits were defined and analysed: body size, molar structure, number of transversal loph(id)s, hypsodonty, horizodonty, presence of acute lophs, presence of obtuse lophs, occlusal topography, degree of enamel folding, skull shape, morphology of upper tusks, morphology of lower tusks, mandible shape, symphyseal

morphology of mandible, pattern of mastication, dental replacement, and foot posture. An extensive description of the traits, their sources, and their ecological relevance is presented in the Supplementary Methods. We collected information to score these traits based on direct observations by several of us (H.Z., M.T.A., J.L.P., and J.S.), and from the literature. The categories of the 17 functional traits are summarised in the Extended Data Fig. 1.

We were able to gather comprehensive ecomorphological information for 180 species and translated 93% of the observed disparity in a two-dimensional NMDS space (by means of a Gower distance matrix; see Supplementary Methods). This allows us to reduce the potential covariation in some of the traits, while making it easier to model ecomorphological evolution in a phylogenetic framework and as part of ecology-dependent models. We also used the Gower distance matrix to compute ecological disparity (measured as the sum of variances), and extinction selectivity over time. Based on the NMDS space, we used *k-means* to identify 8 proboscidean functional types (PFTs). See detailed procedures in the Supplementary Methods. A reconstruction of representative species of the eight PBTs is shown in Figure 1a.

Speciation and extinction rates over time

Detailed fossil occurrence datasets provide the opportunity to estimate speciation and extinction rates through time while controlling for sampling biases. We applied Bayesian procedures (implemented in the software *PyRate*) that analyse occurrence data to simultaneously estimate preservation rates, origination and extinction ages for each species, as well as speciation and extinction rates through time. Complexity in speciation and extinction rates trajectories is modelled by identifying the number of significant rate shifts and their temporal assignment using a reversible jump Markov Chain Monte Carlo (RJMCMC). Temporal ranges associated with each occurrence data point are treated as dating uncertainties, with higher data uncertainty yielding larger uncertainty around parameter estimates. Occurrence ages were randomly resampled 20 times from the uniform distribution defined by their temporal ranges, generating 20 datasets. We run *PyRate* independently on these 20 datasets. The number of generations of the MCMC chains was tailored for each dataset based on exploratory analyses. The MCMC run for the global dataset (including NMDS correlations and a run focussed on the last 10 Myr) was run for 10 million generations. The African, Eurasian and American datasets were run for 5, 7 and 5 million generations, respectively. We sampled every 1000 iterations, and discarded the 10% as burning. The resulting samples obtained from each resampled dataset were enough to ensure ESS above 200 in all key parameters. To report and visualise parameter estimates, 500 random samples were kept from each run, resulting in a total of 10,000 samples from each analysis. Rate shifts were allowed to take place once every million years (the default setting in *PyRate*, `-min_dt 1`). We allowed preservation rates to shift between the Eocene and Oligocene (33.9 Ma), between Aquitanian and the Burdigalian (20.44 Ma), and then for boundaries between these periods: Burdigalian (15.97 Ma) / Serravallian (11.63 Ma) Tortonian / Messinian (5.333 Ma) / Pliocene (2.58 Ma) / Pleistocene (0.0117 Ma)/ Holocene. This definition of boundaries was

aimed at obtaining good posterior estimates of sampling rates and was based on exploratory analyses of occurrence frequency and comparison between different shift configurations.

Detailed diversification profiles for the last 10 Myr were obtained by limiting the *PyRate* analyses (`-edgeShift 10 0`) and allowing rate shifts to take place every 10 kyr (`-min_dt 0.01`), taking advantage of the finer record in Upper Miocene, Pliocene and Quaternary times. The fine timing of extinction shifts for the last 10 Myr was compared to the earliest records of *Homo sapiens* in each continent[48–50] (see Fig. 3a). Importantly, *PyRate* estimates extinction times for all the species, and thus our extinction-rate profiles are not based on a literal reading of last appearance datum (LADs). Our approach is thus conservative regarding the comparison of the timing of extinction shifts with the first records of *Homo sapiens*, since *PyRate* places the timing of the last extinction regime closer to the appearance of modern humans than raw FADs would do.

Finally, we computed diversity curves through time using *PyRate*-implemented functions that combine estimates of sampling rates over time and occurrence distribution, yielding diversity estimates that account for the shifting quality of the paleontological record through time.

Effect of ecology on speciation and extinction

Ecology may exert a very strong impact on diversification rates (speciation and extinction), producing species sorting. To test for a role of ecological function on diversification in Proboscidea, we drew on the possibility to run the Covar model in *PyRate*. Under this model, diversification trajectories are estimated as described above, but each species is able to depart from the overall baseline trend based on a correlation with a continuous variable. In our case, the two axes of our NMDS space were tested for such a correlation. The resulting coefficients (Extended Data Fig. 8) were used to estimate the departure from baseline speciation and extinction for each species (Fig. 2 and Extended Data Fig. 9).

Effect of palaeoclimate on extinction

A major question regarding megaherbivore declines from the Late Miocene onwards is to what extent were species extinctions the results of climatic perturbations. To quantitatively test for an association between the decline of proboscideans (i.e. extinction rates) and palaeoclimate, we use climate-dependent diversification models[14] at the continental level. In order to avoid correlations stemming from broad Cenozoic trends, we restricted our analyses interval to the last 10 Myr. As a proxy for palaeoclimate, we use the recently published record of $\delta^{18}O$ variations in deep-sea benthic foraminifera[41]. We computed two variables from the $\delta^{18}O$ data. We estimated the average $\delta^{18}O$ score in 0.1 Myr bins, as a proxy for temperature (the original data comes with points every 20 kyrs). We also test for a role of the severe short-term environmental fluctuations that characterised the Plio-Pleistocene. To do so, we estimated the absolute of the first differences of the 20 kyrs curve, and then averaged these values into 0.1 bins. Both climate-dependent diversification models were run using the PyRateContinuous.py script in the *PyRate*

software[11] for 1,000,000 generations, sampled the Bayesian search every 1000 iterations, and discarded the first 10% as burnin. Distribution of the correlation parameters for each continent are shown in Figure 3c.

Phylogenetic modelling

We assessed modes of proboscidean ecomorphological evolution using phylogenetic modelling. To do so, we applied the information yielded from the NMDS axes, which are continuous representations of the many functional ecomorphological aspects of proboscideans. Given the multidimensional nature of our data, we used multivariate phylogenetic models[12], which allow us to jointly model the two dimensions of the NMDS space while accounting for the covariance of the axes, as well as their different associated evolutionary rates and/or optimal values.

We fit two sets of models. In the first set, the entire clade is modelled together, and thus represents rates and trends which are shared across all lineages. This set of models include brownian motion (BM), early burst (EB), and Ornstein–Uhlenbeck (OU) stationary model, representing unconstrained diffusion, decaying-rate scenario (e.g. adaptive radiations, ecomorphological stagnation), and constrained or limited evolution, respectively.

In a second set of models, we explore the role of biogeography on the tempo and mode of proboscidean functional evolution. In particular, we investigate the role of the Proboscidean Datum Event (PDE), this is, the dispersal of proboscidean lineages beyond Afro-Arabia at around 22 Ma. In this set of models, we partition the tree in lineages evolving in and outside Africa using functions in the *ape*[51] and *phytools*[52] R packages (see Supplementary Methods), and fit different combinations of the models described above to these two partitions. Further procedural details of models and specific R functions are provided in the Supplementary Methods.

All models were run on 100 trees. The best performing model is the EBBM (EB model in Africa; BM model outside Africa). Parameter estimates and fit of the models are shown in Extended Data Fig. 5.

Trends in community-level proboscidean diversity

We assessed the temporal trends of local species richness and the relationship of averaged dental masticatory durability (DMD; mean NMDS-1 scores) in local richness using mixed-effects models. We tested for the different trends in community richness in four different phases. The African phase spans proboscidean communities before 22 Ma, an age that marks the establishment of several lineages outside Africa (the Proboscidean Datum Event). The second phase, called the after-PDE phase, spans from 22 to 8 Ma. The C_4 expansion phase, includes communities between 8 and 2.4 Ma, reflecting the new ecological settings brought about globally by this new type of grassland biome, which have been previously hypothesised to have a

major impact in megafauna communities[31]. The decline phase spans from 2.4 Ma to the present, reflecting the interval where extinction intensified and drove the clade to its diversity decline.

Models where local species richness was a function of age, and where richness was a function of mean NMDS-1 scores (dental masticatory durability, DMD, which was scaled from 0 to 1, to ease interpretations; see Extended Data Fig. 7b) were evaluated while taking into account age uncertainty and geography-dependent varying effects such as sampling heterogeneity and taxonomic practices (see Supplementary Methods). Mixed effects models were run using the function *lmer* in the R package *lme4*[53]. Corrected Akaike Information Criterion (AICc) scores show that the different phases have an effect both on the slope and the intercepts of the relationships, both for age and DMD models (AICc Weights are 1 in both cases suggesting a strong preference for the most complex models). The parameters of the best models for each variable are provided in Extended Data Fig. 6. A representation of the best models is shown in Extended Data Fig. 7.

Methods references

46. Cantalapiedra, J. L. *et al.* Conserving evolutionary history does not result in greater diversity over geological time scales. *Proc Royal Soc B* **286**, 20182896 (2019).

47. Ronquist, F. *et al.* MrBayes 3.2: Efficient Bayesian Phylogenetic Inference and Model Choice Across a Large Model Space. *Systematic Biol* **61**, 539–542 (2012).

48. Hublin, J.-J. *et al.* New fossils from Jebel Irhoud, Morocco and the pan-African origin of *Homo sapiens*. *Nature* **546**, 289–292 (2017).

49. O'Connell, J. F. *et al.* When did *Homo sapiens* first reach Southeast Asia and Sahul? *Proc National Acad Sci* **115**, 8482–8490 (2018).

50. Ardelean, C. F. *et al.* Evidence of human occupation in Mexico around the Last Glacial Maximum. *Nature* **584**, 87–92 (2020).

51. Paradis, E. *Analysis of Phylogenetics and Evolution with R (Second Edition).* (Springer, 2012).

52. Revell, L. J. phytools: an R package for phylogenetic comparative biology (and other things). *Methods Ecol Evol* **3**, 217–223 (2012).

53. Bates, D., Mächler, M., Bolker, B. & Walker, S. Fitting Linear Mixed-Effects Models Using lme4. *J Stat Softw* **67**, (2015).

54. MacLatchy, L. M., Desilva, J., Sanders, W. J. & Wood, B. Hominini. in *Cenozoic Mammals of Africa* (eds. Werdelin, L. & Sanders, W. J.) 471–545 (University of California Press, 2010).

Acknowledgements: We thank D. Silvestro, J. Calatayud and J. Clavel for technical assistance, and F. Bibi, M.J. Benton and W.J. Sanders for helpful comments. S. Wang and G. van den Bergh provided important constructive comments on the informal supertree. Gratitudes are extended to E.M. Dunne, D. Mothé, F. Rivals and two other anonymous reviewers, whose comments and recommendations improved the presentation of this paper. This is PBDB publication #398.

Funding: This work was supported by the Talent Attraction Program of the Madrid Government (2017-T1/AMB5298), the German Research Foundation (DFG, AOBJ: 637491), and the Academy of Finland (post-doctoral research fund nr. n:o 315691).

Author contributions: J.L.C., O.S. and J.S. conceptualised the research. J.L.C, O.S., J.S., H.Z., M.T.A. and J.L.P. gathered the data. J.L.C., O.S. and F.B. designed and performed the analysis. J.S. wrote the description and relevance of functional traits. J.L.C. and O.S. wrote the first version of the paper, and H.Z. and J.S. contributed to the final version (main text and supplement).

Competing interests: Authors declare no competing interest.

Data and materials availability: Datasets are available in the Supplementary Data file 1 and *FigShare* (doi: 10.6084/m9.figshare.14035109).

Code availability: *PyRate* is a Python v.3. based program available at https://github.com/dsilvestro/PyRate. Computation in R used functions in packages *mvMORPH*, *phytools*, *ape* and *lme4*. Input files can be obtained from Supplementary Data file 1 and from *FigShare* (doi: 10.6084/m9.figshare.14035109).

Figure 1. Ecological diversity and diversification in proboscideans. a, Reconstruction of representative genera for the eight proboscidean functional types (PFTs), including their upper third molars (molars not shown to scale). **PFT 1** *Moeritherium* – sublophodont molar with distinct cusps; **PFT 2** *Deinotherium* - bilophodont molar with crenulated ridges; **PFT 3** *Gomphotherium* - longirostrine mandible with pronounced lower incisors, basic bunodont molar with rounded cusps; **PFT 4** *Mammut* - brevirostrine mandible with lower incisors extremely vestigial or absent; zygodont molar (with ridged cusps); **PFT 5** *Amebelodon* - longristrine mandible with shovel-shaped lower incisors, bunolamellar molar; **PFT 6** *Anancus* - brevirostrine mandible with lower incisors lost, complex bunodont molar achieving enhanced DMD; **PFT 7** *Stegodon* - brevirostrine mandible lacking lower incisors, brachydont (low-crowned) proal shearing molar comprising of numerous lamellae; **PFT 8** *Palaeoloxodon* - brevirostrine mandible lacking lower incisors, hypsodont (high-crowned) proal shearing molar comprising of numerous lamellae adjoined together by cementum. **b**, Two-dimensional functional space with colour-coded assignation to PFTs based on our 17 ecomorphological traits. **c**, species diversity of the PTFs through time (log-scaled), showing the timing of the PDE (grey bar), and ecological disparity, measured as the sum of variances. **d**, Global and continental speciation and extinction rates through time; rates are log-scaled; shaded areas represent 95% credible intervals. Artwork by O.S..

Figure 2. Effect of ecomorphology on diversification. Ecomorphology-predicted departure of speciation (**a**), and extinction (**b**). These are derived from the correlations of rates with NMDS axes. Based on the NMDS scores of each species, we can plot their expected departure from baseline rates on the NMDS space and the proboscidean phylogeny (see also Extended Data Fig. 8 and 9). The central vertical bar represents PFT assignment.

Figure 3. Extinction trends in the last 10 Myr. a, Continental extinction rates through time on log-scaled axes, where triangles mark the timings at which earlier presence of *Homo sapiens* sensu lato[54] became established on the respective landmasses (Africa 315

602 kya; Eurasia 55 kya; Americas 30 kya) [48–50]. **b**, Extinction selectivity shows whether
603 extinction is ecologically-restricted (positive values) or hits on broad regions of the
604 functional space (negative values); the grey band represents values consistent with a
605 random signal (non-significant *P*-values). **c**, posterior distributions of correlation
606 parameters of extinction with paleotemperature trends for each continent; horizontal
607 bars show the 95 highest probability density.

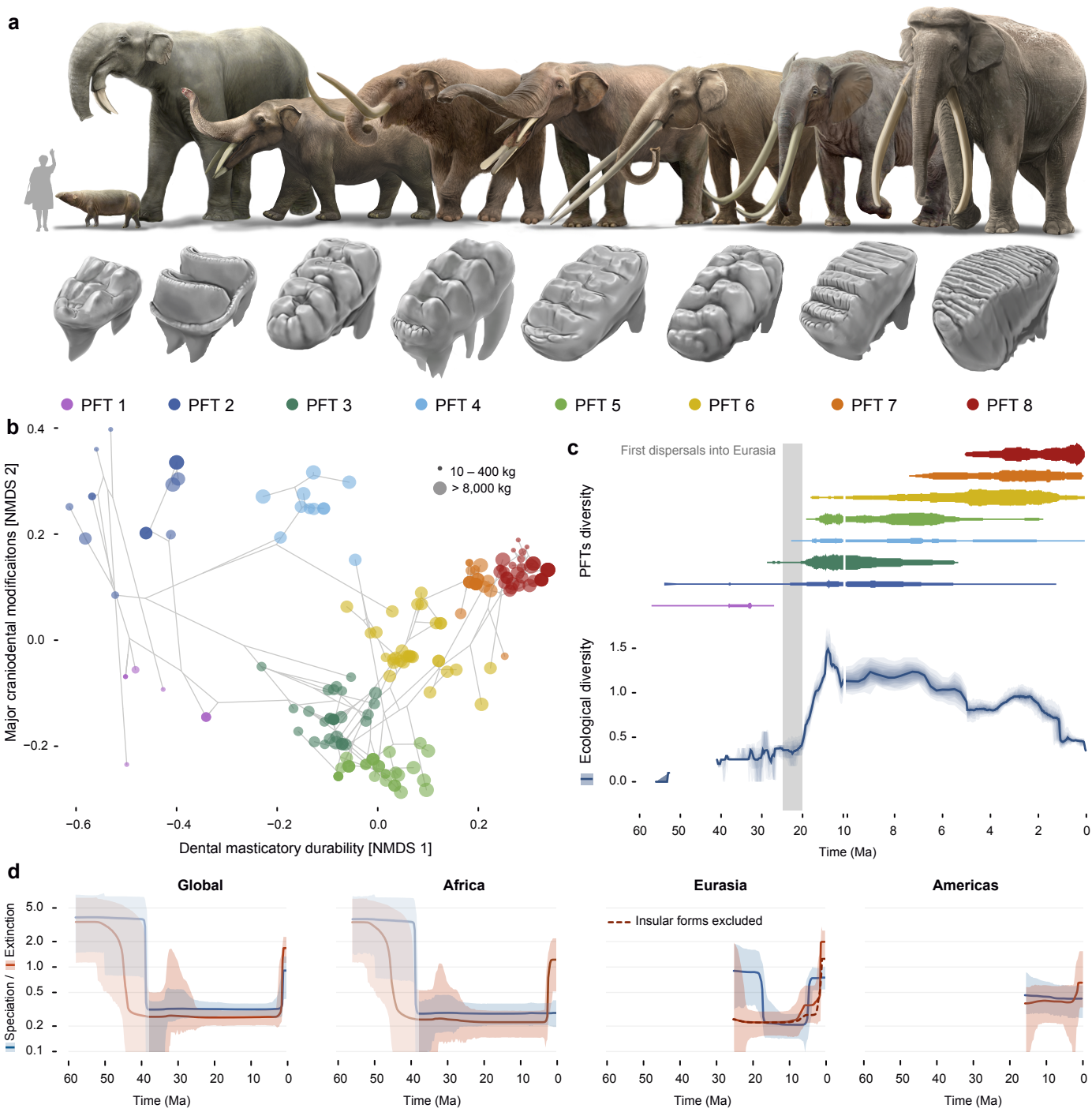
a
PFT 1
PFT 2
PFT 3
PFT 4
PFT 5
PFT 6
PFT 7
PFT 8
b
Major craniodental modificaitons [NMDS 2]
Dental masticatory durability [NMDS 1]
10 – 400 kg
> 8,000 kg
c
First dispersals into Eurasia
PFTs diversity
Ecological diversity
Time (Ma)
d
Global
Africa
Eurasia
Americas
Insular forms excluded
Speciation / Extinction
Time (Ma)

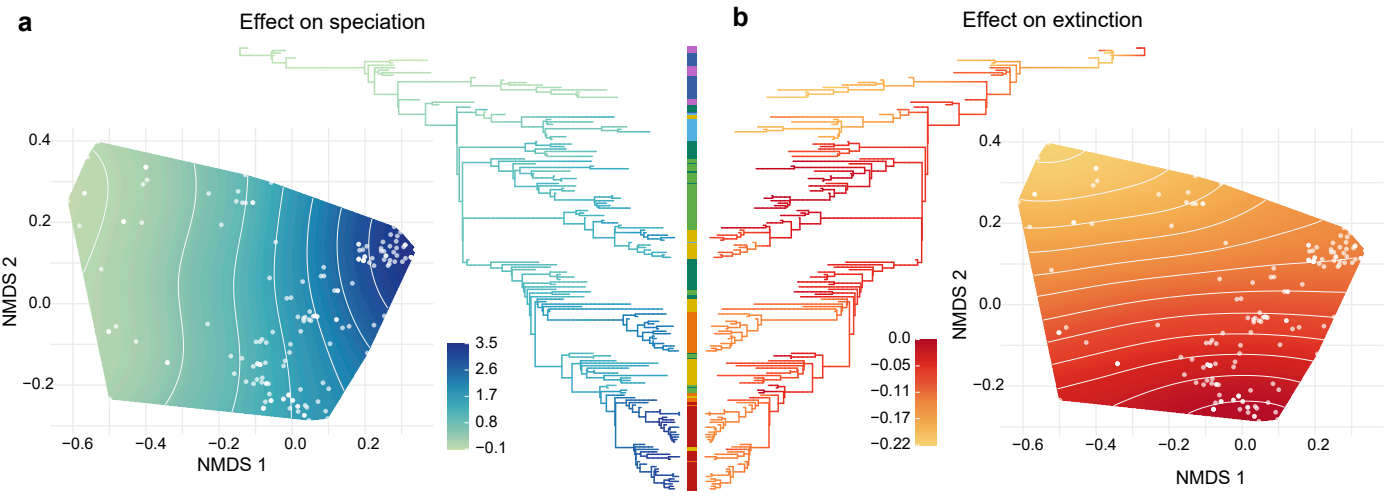
a
Effect on speciation
NMDS 2
NMDS 1
0.4
0.2
0.0
−0.2
−0.6
−0.4
−0.2
0.0
0.2
3.5
2.6
1.7
0.8
−0.1
b
Effect on extinction
NMDS 2
NMDS 1
0.4
0.2
0.0
−0.2
−0.6
−0.4
−0.2
0.0
0.2
0.0
−0.05
−0.11
−0.17
−0.22

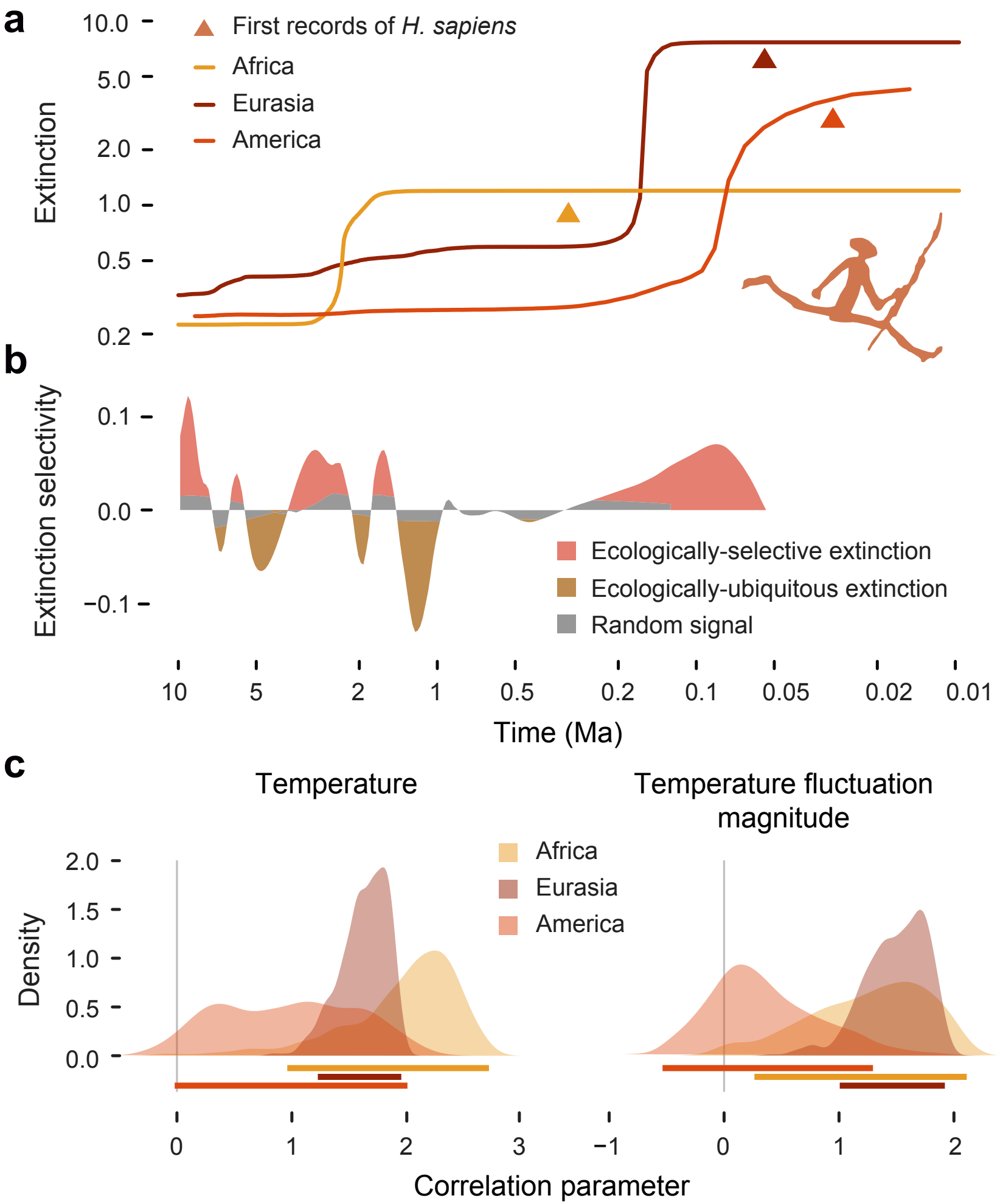
a
10.0
5.0
2.0
1.0
0.5
0.2
Extinction
First records of H. sapiens
Africa
Eurasia
America
b
0.1
0.0
−0.1
Extinction selectivity
Ecologically-selective extinction
Ecologically-ubiquitous extinction
Random signal
10
5
2
1
0.5
0.2
0.1
0.05
0.02
0.01
Time (Ma)
c
Temperature
Temperature fluctuation magnitude
Africa
Eurasia
America
2.0
1.5
1.0
0.5
0.0
Density
0
1
2
3
−1
0
1
2
Correlation parameter

Trait	levels	order
tooth type	1: bunodont 2: bilophodont 3: buno-lamellar 4: lamellar 5: zygodont	unordered
number of transversal lophs	0: 0 lophs 1: 2 lophs 2: 3 lophs 3: 4 - 5 lophs 4: 6 – 7 lophs 5: 8 – 9 lophs 6: 10 – 14 lophs 7: more than 14 lophs	ordered
presence of acute lophs	0: absent 1: present	unordered
presence of obtuse lophs	0: absent 1: present	unordered
occlusal topography	0: raised elements 1: flat	unordered
hypsodonty	0: brachyodont 1: mesodont 2: hypsodont	ordered
horizodonty	1: 2 cusps pairs 2: 3 cusps pairs 3: 4 - 5 cusps pairs 4: 6 – 7 cusps pairs 5: 8 – 9 cusps pairs 6: 10 – 14 cusps pairs 7: more than 14 cusps pairs	ordered
enamel folding	0: absent 1: present	unordered
body size	1: 10-400 kg 2: 400 - 1000 kg 3: 1000 - 2000 kg 4: 2000 - 3000 kg 5: 3000 - 5000 kg 6: 5000 - 8000 kg 7: > 8000 kg	ordered
skull shape	0: non-specialised (e.g. *Eritherium*, *Phosphatherium*) 1: non-bathycephalic, flat (e.g. *Deinotheriidae*, *Palaeomastodon*, *Choerolophodon*) 2: non-bathycephalic, domed (e.g. *Gomphotherium*, *Afrochoerodon*) 3: bathycephalic, non-hypsicephalic (e.g. *Loxodonta*, *Stegodon*) 4: bathycephalic, hypsicephalic (e.g. *Elephas*, *Mammuthus*)	unordered
upper tusks	0: I2s with generalised incisor-like morphology (e.g. *Phosphatherium*) 1: I2s hippo-like (e.g. *Moeritherium*) 2: down-curved (e.g. *Gomphotherium*, *Platybelodon*, *Eozygodon*) 3: nearly straight, very little down or up-curve (e.g. *Cuvieronius*, *Anancus*, *Stegotetrabelodon*) 4: gentle up-curve (e.g. *Mammut americanum*, *Loxodonta*, *Elephas*) 5: very strong up-curve (e.g. *Mammuthus*, *Choerolophodon corrugatus*) 6: lost/absent, no evidence of functional role (*Prodeinotherium hobleyi*)	unordered
lower tusks	0: short, i2 always present (e.g. *Phosphatherium*, *Moeritherium*) 1: developed, conical or oval in section, straight or curved (e.g. *Omanitherium*, *Gomphotherium*, *Deinotherium*) 2: developed and flattened, shovel-like (e.g. *Amebelodon*, *Platybelodon*) 3: absent or very reduced (e.g. *Mammut*, *Primelephas*, *Loxodonta*).	unordered
mandible	0: short with great angle of ventral deflection (*Prodenotherium*, *Deinotherium*) 1: long and straight (relative to the occlusal border; e.g. *Gomphotherium*, *Konobelodon*) 2: long with great angle of ventral deflection (e.g. *Stegotetrabelodon*, *Tetralophodon*) 3: short and with missing or reduced lower tusks (e.g. *Mammut*, *Elephas*)	unordered
mandibular symphysis	0: reduced, with or without incisors (earliest taxa, *Elephas*) 1: long, with parallel borders (e.g. *Konobelodon*, *Tetralophodon*, *Gomphotherium stenheimense*, *Deinotherium*) 2: long and rostrally broadened (e.g. *Amebelodon*, *Protanancus*, *Platybelodon*, *Gomphotherium angustidens*)	unordered
pattern of mastication (POM)	0: Deinotherium-pattern of mastication (e.g. *Deinotherium*, *Numidotherium*, *Phosphatherium*) 1: Gomphotherium-pattern of mastication (e.g. *Gomphotherium*) 2: Mammutian-pattern of mastication (e.g. *Mammut*, *Zygolophodon*) 3: Elephantian-pattern of mastication (e.g. *Elephas*, *Stegodon*, *Mammuthus*)	unordered
teeth replacement	0: P4/p4 present when M3/m3 in function 1: P4/p4 absent when M3/m3 in function.	unordered
foot posture	0: plantigrade 1: subunguligrade	unordered

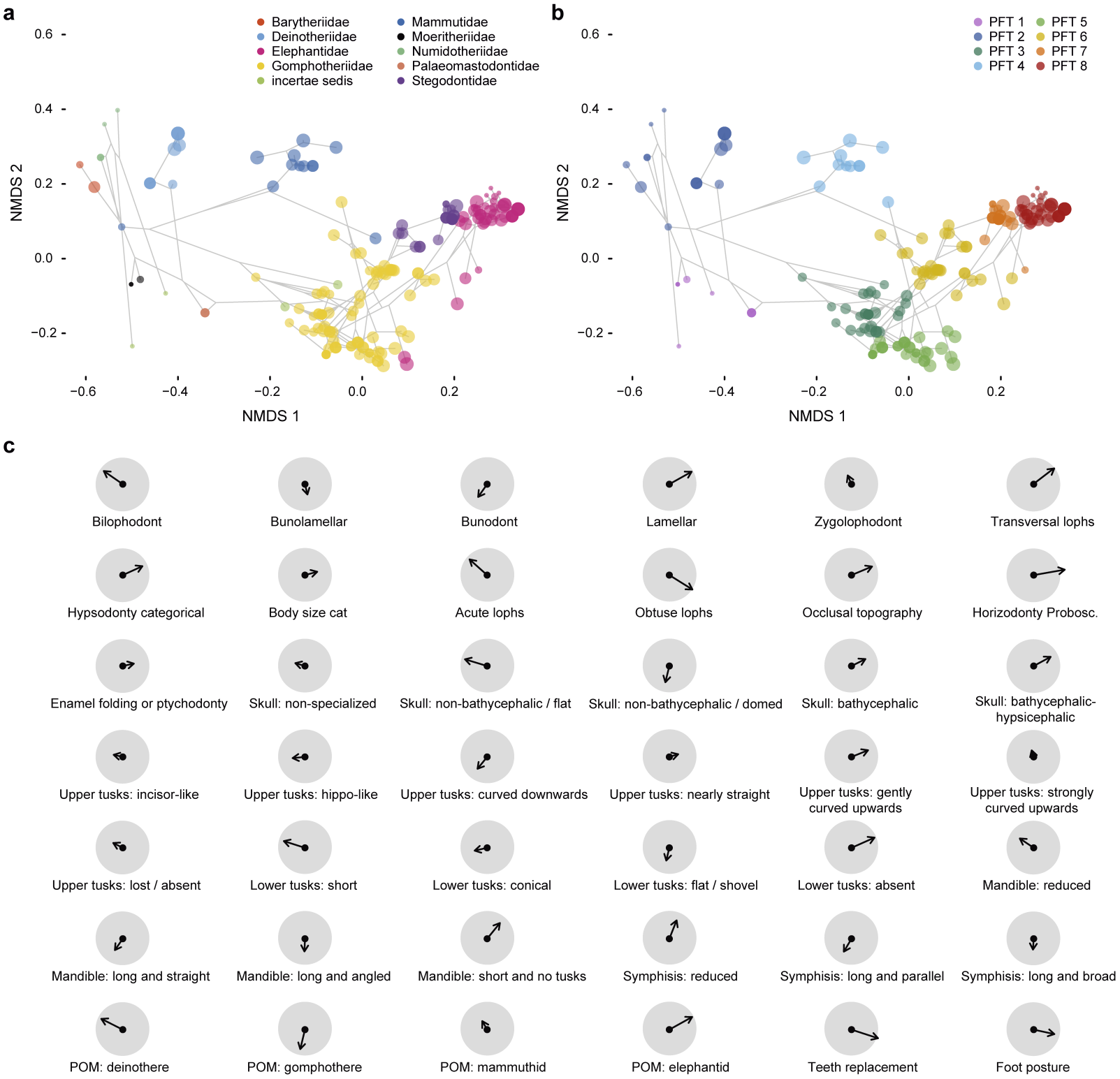
a
Barytheriidae
Deinotheriidae
Elephantidae
Gomphotheriidae
incertae sedis
Mammutidae
Moeritheriidae
Numidotheriidae
Palaeomastodontidae
Stegodontidae
NMDS 1
NMDS 2
b
PFT 1
PFT 2
PFT 3
PFT 4
PFT 5
PFT 6
PFT 7
PFT 8
NMDS 1
NMDS 2
c
Bilophodont
Bunolamellar
Bunodont
Lamellar
Zygolophodont
Transversal lophs
Hypsodonty categorical
Body size cat
Acute lophs
Obtuse lophs
Occlusal topography
Horizodonty Probosc.
Enamel folding or ptychodonty
Skull: non-specialized
Skull: non-bathycephalic / flat
Skull: non-bathycephalic / domed
Skull: bathycephalic
Skull: bathycephalic-hypsicephalic
Upper tusks: incisor-like
Upper tusks: hippo-like
Upper tusks: curved downwards
Upper tusks: nearly straight
Upper tusks: gently curved upwards
Upper tusks: strongly curved upwards
Upper tusks: lost / absent
Lower tusks: short
Lower tusks: conical
Lower tusks: flat / shovel
Lower tusks: absent
Mandible: reduced
Mandible: long and straight
Mandible: long and angled
Mandible: short and no tusks
Symphisis: reduced
Symphisis: long and parallel
Symphisis: long and broad
POM: deinothere
POM: gomphothere
POM: mammuthid
POM: elephantid
Teeth replacement
Foot posture

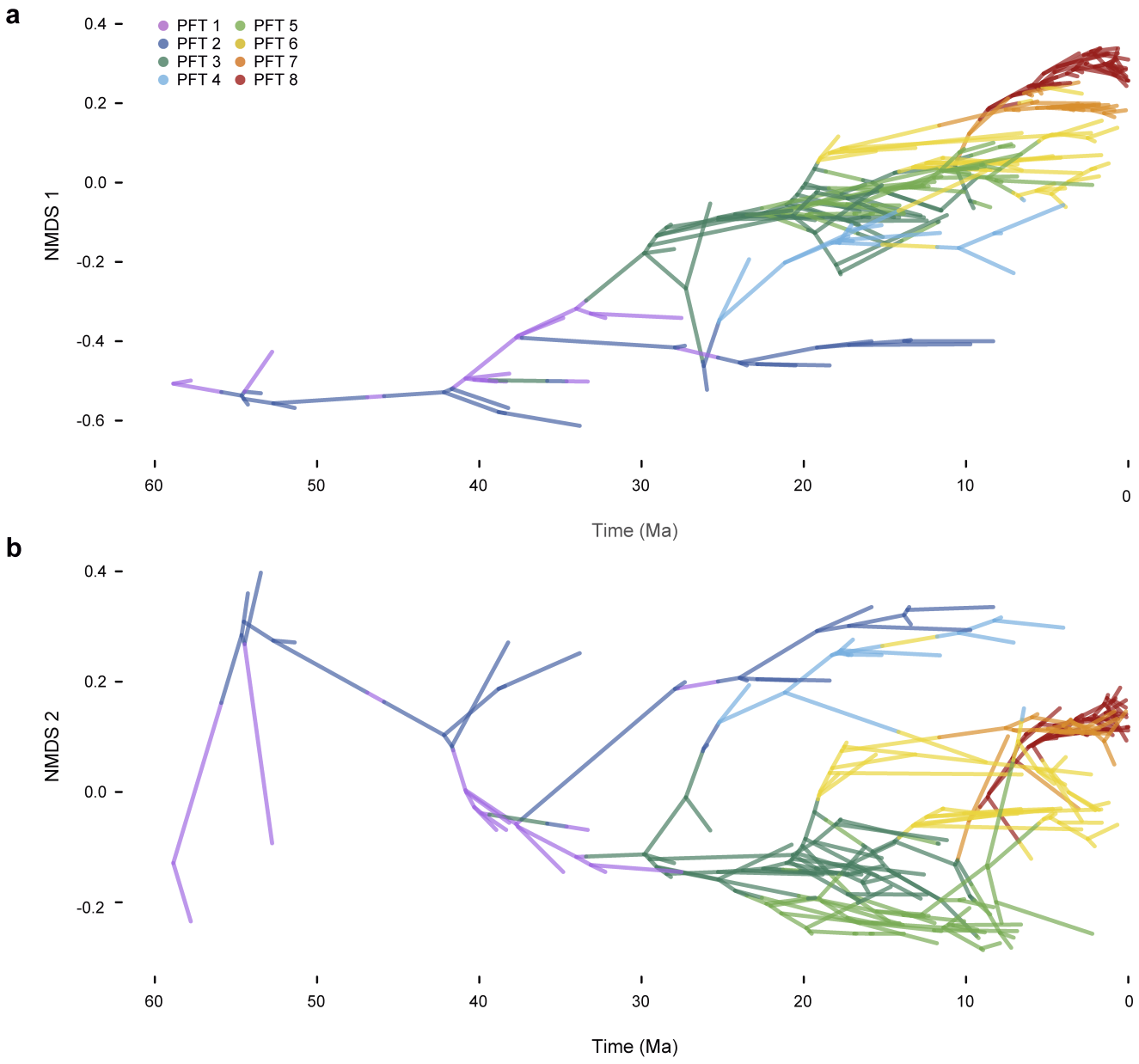
a
PFT 1
PFT 2
PFT 3
PFT 4
PFT 5
PFT 6
PFT 7
PFT 8
NMDS 1
0.4
0.2
0.0
-0.2
-0.4
-0.6
60
50
40
30
20
10
0
Time (Ma)
b
NMDS 2
0.4
0.2
0.0
-0.2
60
50
40
30
20
10
0
Time (Ma)

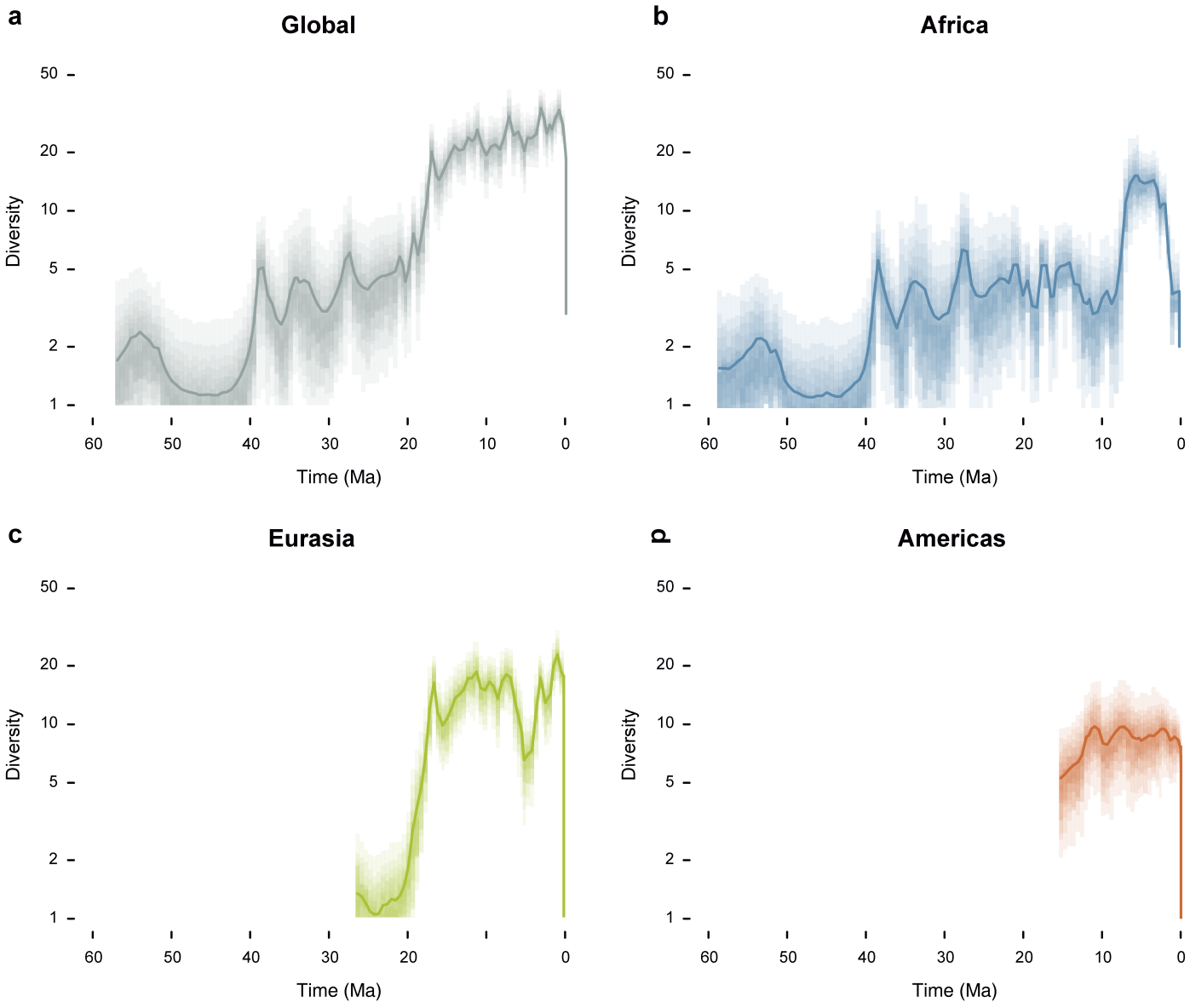
a
Global
b
Africa
c
Eurasia
d
Americas
Diversity
Time (Ma)
50
20
10
5
2
1
60
50
40
30
20
10
0

Africa

	AICc Weights	AICc	root NMDS1	root NMDS-2	rate NMDS-1	rate NMDS-2	correlation between rates	rate decay (EB)	attraction NMDS1 [OU]	attraction NMDS2 [OU]	optimum NMDS-1 [OU]	optimum NMDS2 [OU]
EBBM	0.465	-894.71	-0.510	-0.071	0.001	0.001	0.000	-0.069	-	-	-	-
EBOU	0.447	-894.63	-0.510	-0.071	0.001	0.001	0.000	-0.068	-	-	-	-
EB	0.088	-891.38	-0.509	-0.073	0.014	0.019	0.002	-0.054	-	-	-	-
BMEB	0.000	-865.82	-0.509	-0.078	0.002	0.005	-0.001	-	-	-	-	-
BM shifting rate	0.000	-864.82	-0.509	-0.078	0.002	0.005	-0.001	-	-	-	-	-
OU	0.000	-796.31	-0.534	-0.085	0.001	0.003	0.000	-	0.013	0.035	26.285	-13.519
OU shifting optima	0.000	-796.20	-0.536	-0.094	0.001	0.003	0.000	-	0.008	0.038	236.381	-8.326
BM	0.000	-785.75	-0.509	-0.078	0.001	0.003	0.000	-	-	-	-	-

outside Africa

	attraction NMDS1 [OU]	attraction NMDS2 [OU]	rate NMDS-1	rate NMDS-2	correlation between rates	rate decay [EB]	optimum NMDS-1 [OU]	optimum NMDS-2 [OU]	correlation of attraction parameter
EBBM	-	-	0.027	0.026	-0.002	-	-	-	-
EBOU	0.045	0.043	0.027	0.026	-0.002	-	-0.510	-0.071	-0.035
EB	-	-	-	-	-	-	-	-	-
BMEB	-	-	0.001	0.001	0.000	-0.022	-	-	-
BM shifting rate	-	-	0.002	0.005	-0.001	-	-	-	-
OU	-	-	-	-	-	-	-	-	0.006
OU shifting optima	0.008	0.038	-	-	-	-	89.023	-3.393	0.008
BM	-	-	-	-	-	-	-	-	-

	phase	mean intercept	lower CI	upper CI	mean slope	lower CI	upper CI
richnes ~age*phase	African phase 60 - 22 Ma	0.687	0.459	0.916	-0.003	-0.007	0.001
	After PDE 22 - 8 Ma	1.505	1.304	1.706	0.013	0.008	0.017
	C_4 expansion 8 - 2.4 Ma	1.615	1.417	1.814	-0.047	-0.055	-0.039
	Decline 2.4 - 0 Ma	1.694	1.490	1.899	-0.039	-0.046	-0.032
richnes ~mean_DMD*phase	African phase 60 - 22 Ma	0.723	0.486	0.959	-0.055	-0.232	0.122
	After PDE 22 - 8 Ma	1.399	1.183	1.615	0.209	0.175	0.243
	C_4 expansion 8 - 2.4 Ma	1.538	1.323	1.754	-0.156	-0.193	-0.119
	Decline 2.4 - 0 Ma	1.617	1.400	1.834	-0.196	-0.225	-0.166

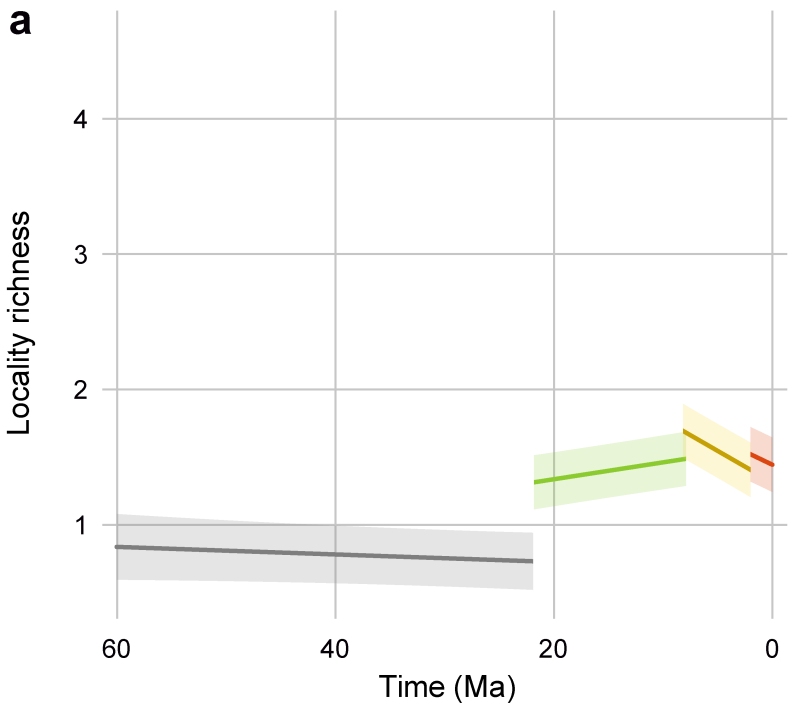

Richness ~ age * phase

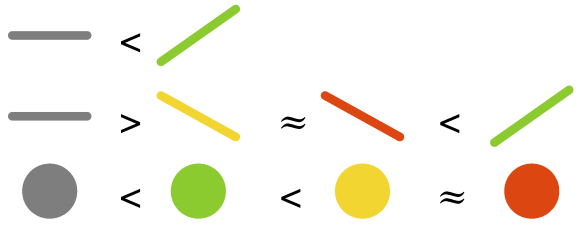

Phase

- A: African phase (60 – 22 Ma)
- B: After Proboscidean Datum Event (22 – 8 Ma)
- C: C_4 Expansion phase (8 – 2.4 Ma)
- D: Decline phase (2.4 – 0 Ma)

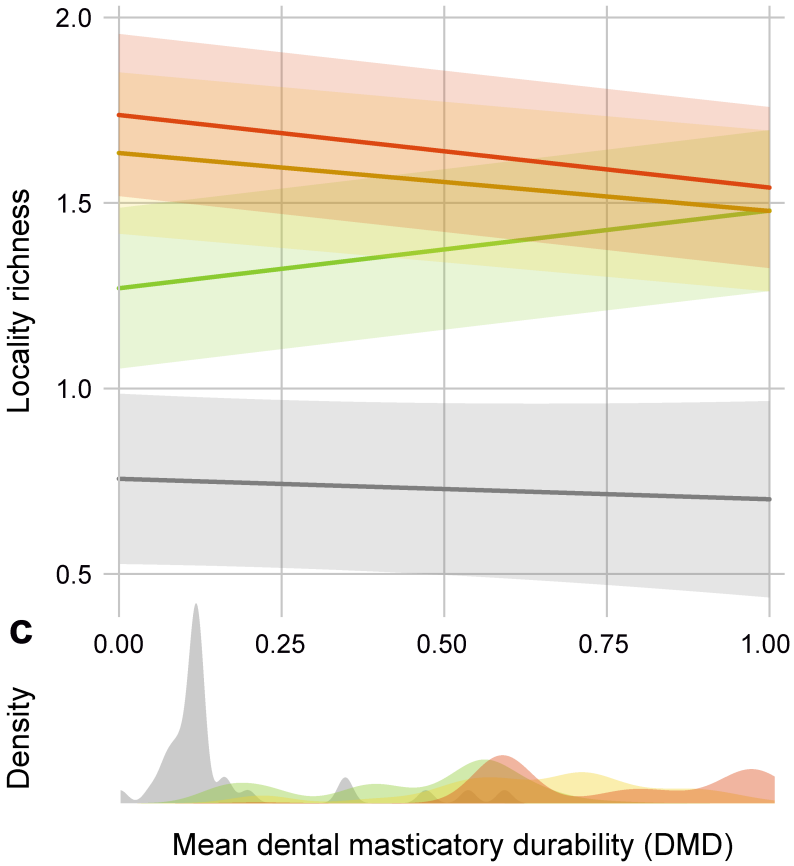

Richness ~ Mean DMD * phase

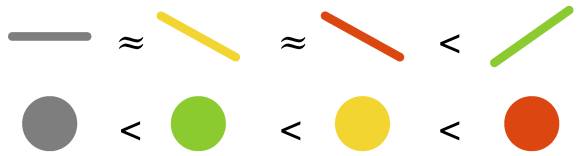

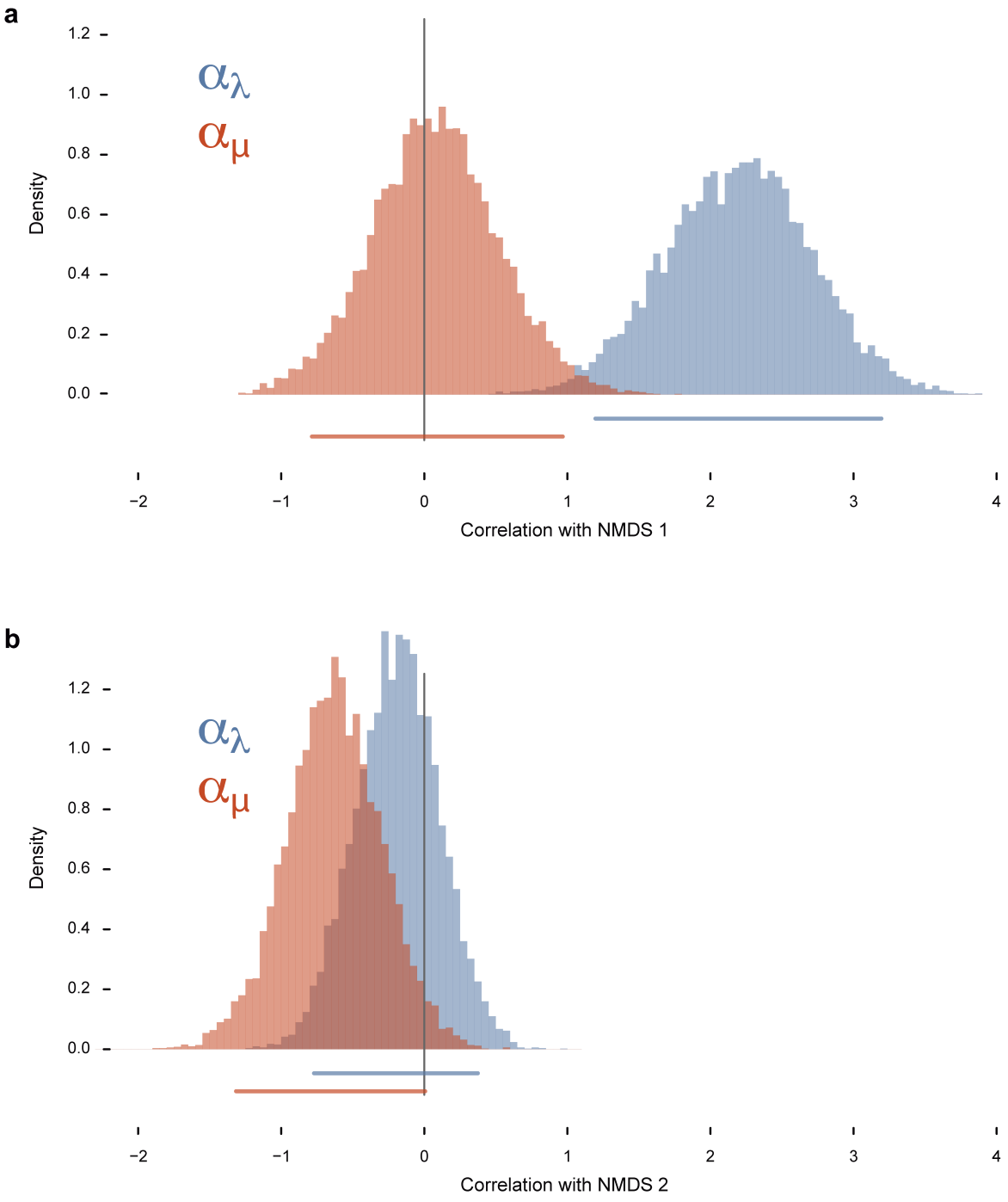
a
1.2
1.0
0.8
0.6
0.4
0.2
0.0
Density
α_λ
α_μ
−2
−1
0
1
2
3
4
Correlation with NMDS 1
b
1.2
1.0
0.8
0.6
0.4
0.2
0.0
Density
α_λ
α_μ
−2
−1
0
1
2
3
4
Correlation with NMDS 2

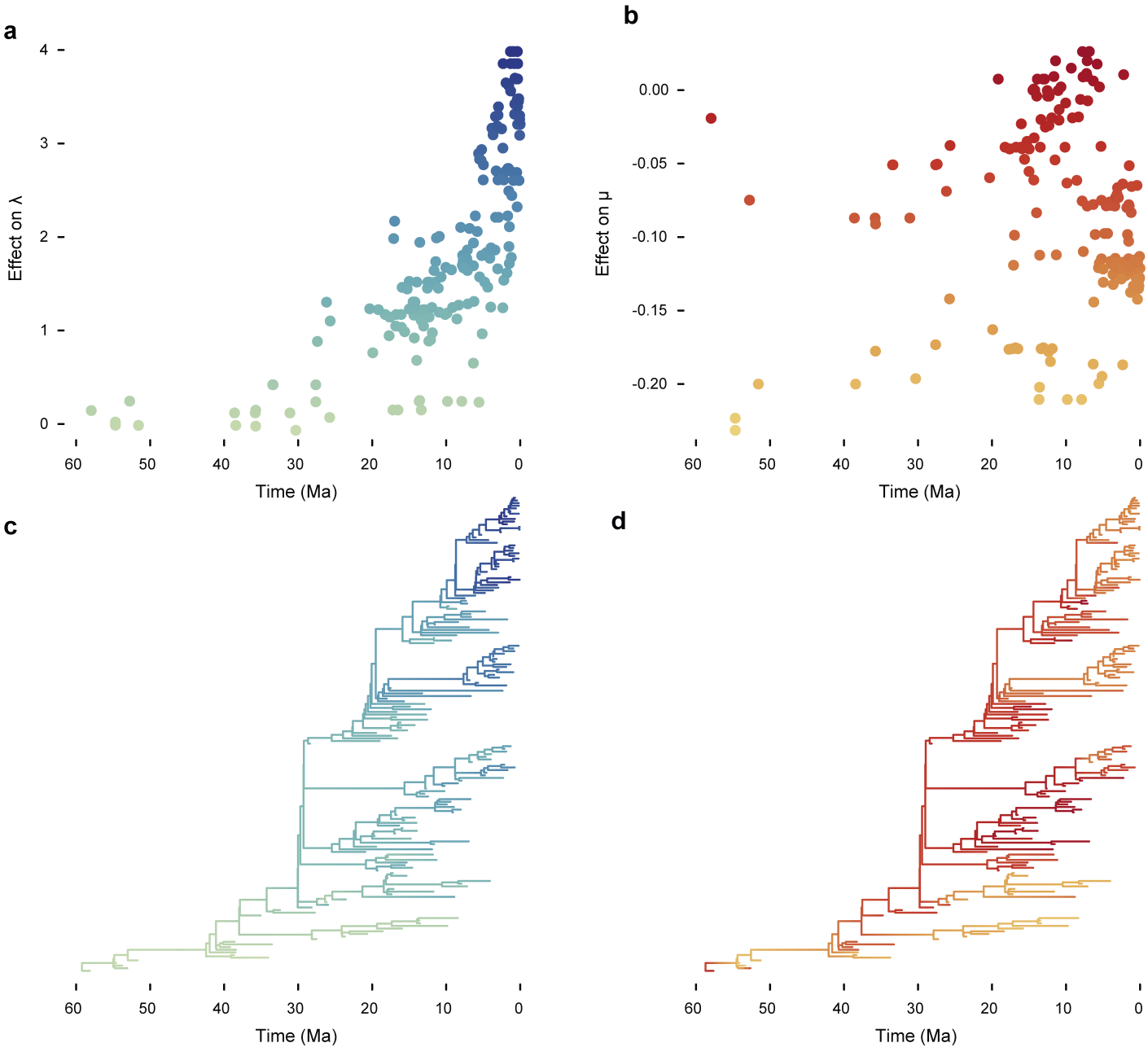
a
Effect on λ
4
3
2
1
0
60
50
40
30
20
10
0
Time (Ma)
b
Effect on μ
0.00
-0.05
-0.10
-0.15
-0.20
60
50
40
30
20
10
0
Time (Ma)
c
60
50
40
30
20
10
0
Time (Ma)
d
60
50
40
30
20
10
0
Time (Ma)

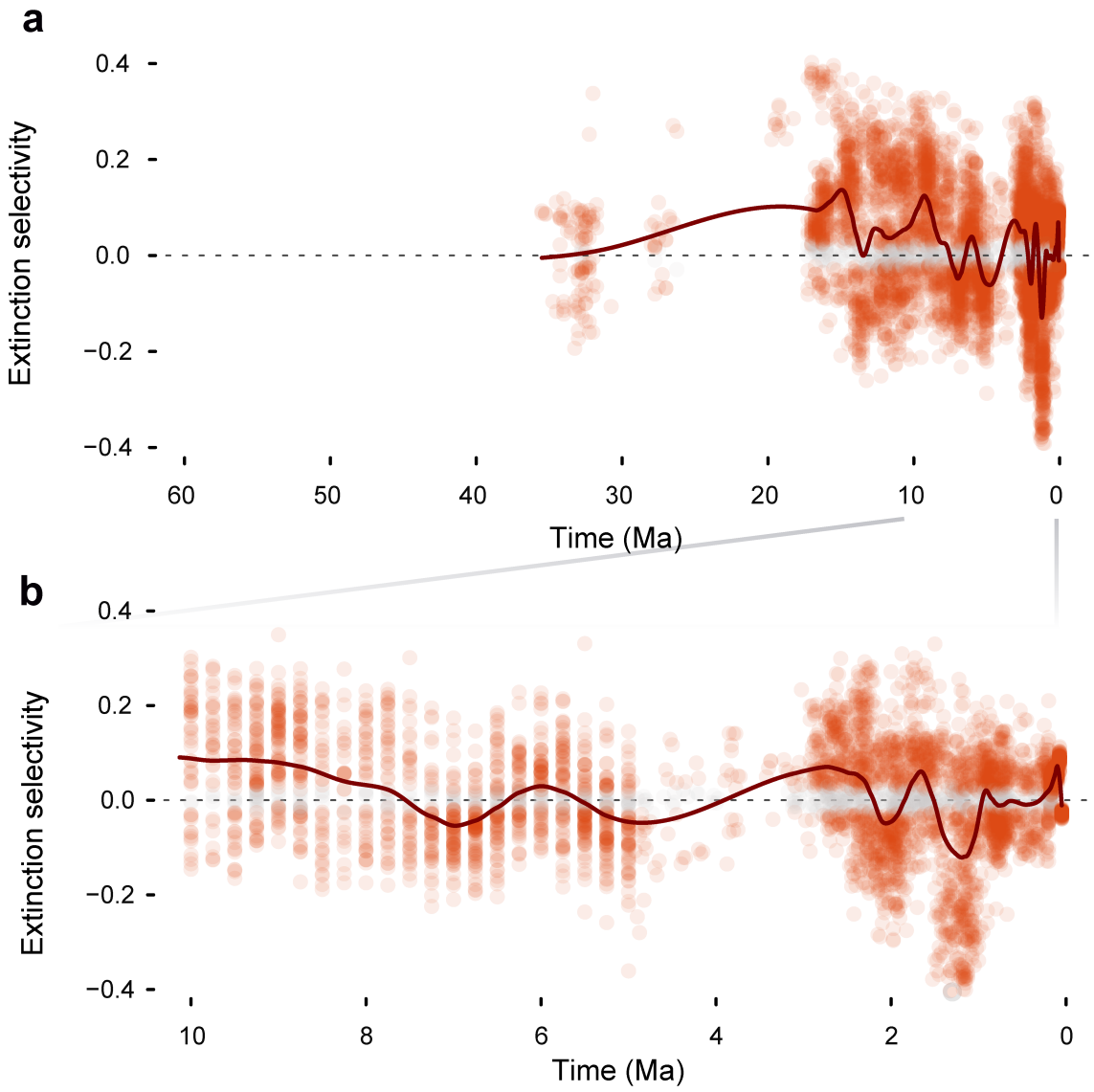
a
0.4
0.2
0.0
−0.2
−0.4
Extinction selectivity
60
50
40
30
20
10
0
Time (Ma)
b
0.4
0.2
0.0
−0.2
−0.4
Extinction selectivity
10
8
6
4
2
0
Time (Ma)